An Efficient and Eco-Friendly Solution-Chemical Route for Preparation of Ultrastable Reduced Graphene Oxide Suspensions

Dafang He, Liming Shen, Xiaoyan Zhang, Yifeng Wang, and Ningzhong Bao
State Key Laboratory of Material-Oriented Chemical Engineering, Dept. of Chemical Engineering, College of Chemistry and Chemical Engineering, Nanjing Tech University, Nanjing, Jiangsu 210009, P.R. China

Harold H. Kung
Dept. of Chemical and Biological Engineering, Northwestern University, Evanston, IL 60208

DOI 10.1002/aic.14499
Published online May 29, 2014 in Wiley Online Library (wileyonlinelibrary.com)

We describe a facile and eco-friendly solution approach to chemically reduce graphene oxide (GO) to high-quality graphene using nontoxic inexpensive reductants. The reduction process and mechanism of a group of eco-friendly reductants were systematically studied. These reductants perform quite differently in terms of reduction rate (L-ascorbic acid [L-AA] > D-fructose > sucrose > glucose > sodium sulfite), density of small sp^2 domains (L-AA > sodium sulfite > glucose > sucrose > D-fructose), degree of reduction (L-AA > glucose > D-fructose > sodium sulfite > sucrose), and stability of the reduced GO suspension (L-AA > D-fructose > sucrose > glucose > sodium sulfite). L-AA shows the highest reducing ability, achieving the largest extent of reduction after 10 min in the presence of ammonia. Both residual oxygen functionalities and the adsorbed oxidization products of L-AA on the graphene surface are responsible for stabilizing the reduced GO suspension over several months. © 2014 American Institute of Chemical Engineers *AIChE J*, 60: 2757–2764, 2014
Keywords: graphene oxide, graphene, L-ascorbic acid, reducing ability, solution-chemical method

Introduction

Graphene, a two-dimensional (2-D) monolayer of carbon atoms with a honeycomb crystal lattice, has attracted significant attention owing to its unusual electronic, thermal, and mechanical properties.[1–3] This 2-D material holds great promise for potential applications in many technological fields such as nanoelectronics,[4] composite materials,[5,6] gas sensors,[7,8] and energy storage devices.[9–13] To realize these practical applications, suitable synthetic methods are needed to produce high-quality graphene on a large scale and at low cost. So far, methods to prepare graphene include micromechanical exfoliation,[14] chemical vapor deposition,[15] epitaxial growth,[16,17] cutting carbon nanotubes,[18,19] sonication,[20] and solution-chemical reduction of graphene oxide (GO).[21,22] However, the low efficiency or high cost of these methods has limited their applicability to research laboratories. Comparatively, solution-chemical reduction is preferable among these methods because it is scalable and capable of generating numerous chemical functionalities useful for subsequent surface modification and eventual practical applications. The drawback of this method, however, lies in the toxicity of the reductants used and facile agglomeration of chemically reduced GO sheets that can be redispersed only after significant effort. Typically, strong reductants such as hydrazine/hydrazine derivatives[23–25] and sodium borohydride, have been used to reduce GO to form high-quality-reduced GO.[26] They are highly toxic and potentially explosive, which are undesirable in large-scale preparation and practical applications. Although reduced GO sheets have a high-specific surface area, their hydrophobic nature causes them to rapidly agglomerate in aqueous solutions and some organic solvents, and, in some cases, even restack to form graphite through van der Waals interactions.[27] Therefore, it is highly desirable to identify a safe, inexpensive, and efficient reductant for the development of scalable solution-chemical routes to prepare high-quality-reduced GO with good dispersibility in solvents.

Several eco-friendly, nontoxic, inexpensive, and strong reductants, such as L-ascorbic acid (L-AA, a form of vitamin C), D-fructose, glucose, sucrose, and sodium sulfite (Na_2SO_3), have been widely used for both laboratory and industrial applications. For example, Na_2SO_3 is a common bleaching agent in food and dye industries.[28] Reducing sugars (such as D-fructose, glucose, and sucrose) have been widely used in the food, medical, and mirror industry.[29] L-AA has been used for fruit and vegetable processing to make the products appear more brilliant and fragrant.[30] Recently, the utilization of these eco-friendly and low-cost reductants have been extended to graphene preparation. A

Additional Supporting Information may be found in the online version of this article.

Correspondence concerning this article should be addressed to L. Shen at lshen@njtech.edu.cn or N. Bao at nzhbao@njtech.edu.cn.

Conflict of interest: The authors declare no conflict of interest associated with this work.

handful of reports demonstrated their use to reduce GO in laboratories. For example, Chen et al. produced highly conductive graphene using Na_2SO_3 as reductant.[31] Gao et al. used L-AA to reduce GO in the presence of L-tryptophan as the stabilizer to prepare a colloidal suspension of electrically conducting graphene.[32] These studies have shown the feasibility of eco-friendly solution-chemical reduction approach to prepare reduced GO. Herein, we report our systematic investigation of the performance of five eco-friendly and inexpensive reductants (including L-AA, D-fructose, glucose, sucrose, and Na_2SO_3) in the presence of ammonia for the reduction of GO. A very efficient route to produce high-quality-reduced GO has been developed. Particularly, the resulting reduced GO can be readily dispersed in either polar or nonpolar solvents for subsequent potential applications such as composites, conductive coatings/paints/inks, biomedicine, energy storage, and conversion.

Experimental

Materials

All the chemicals, including natural flake graphite (Qingdao Huatai Lubricant Ltd.), D-fructose (Xilong Chemical Ltd.), sucrose (Huixing Biochemical Reagent Ltd.), L-AA, sodium sulfite, and glucose (the latter three were purchased from Sinopharm Chemical Reagent) were used as-received without further purification.

Synthesis of GO

GO was synthesized from natural flake graphite using a modified Hummers method.[33] Natural flake graphite (1.0 g), with an average particle size of 83 mesh (181 μm), and potassium nitrate (1.5 g) were mixed in sulfuric acid (50 mL, 98 wt%) with stirring, and the mixture was cooled in an ice bath. Potassium permanganate (6.0 g) was slowly added to the above mixture with vigorous stirring for both improved mixing with the graphite and maintaing the temperature below 20°C. The mixture was then heated at 45°C for 2 h in a water bath, forming a thick paste. Water of 100 mL was gradually added into the paste with continuously stirring at 90°C for 10–20 min. Additional 200 mL water was subsequently added into the mixture in a similar fashion. Finally, the mixture was treated with 10 mL H_2O_2 (30 wt%), turning the color of the solution from dark brown to yellow. The mixture was repeatedly centrifuged and washed with DDI water until the pH of the solution became neutral. The resulting graphite oxide was dried in air and then dispersed in water to form a suspension. Exfoliation of graphite oxide to a homogeneous GO suspension was achieved by gently shaking the graphite oxide suspension for 12 h.

Chemical reduction of GO

In a typical procedure, 1.4 mmol L-AA was first added into a 25 mL GO suspension (1 mg/mL), and then 20 μL of ammonia solution (25% w/w) was added. The mixture was vigorously shaken for a few minutes and then stirred at 95°C for more than 10 min. The mixture was subsequently cooled to room temperature and the resulting stable black suspension was centrifuged at 3000 rpm and washed with water three times. The obtained reduced GO sheets were redispersed in water and stored before further processing. As for the reduction of GO by the other four reductants, 1.4 mmol D-fructose, 0.7 mmol sucrose, 2.2 mmol glucose, and 2.3 mmol sodium sulfite were used in reactions with times of 30 min, 1 h, 1 h, and 4 h, respectively, without changing the rest of the procedure.

Characterizations

The UV-Vis absorption spectra were collected using a CARY 5000 spectrophotometer. Aqueous suspensions of sample powders (~0.05 mg/mL) and reference pure water were used for measurements. Fourier transform infared (FT-IR) spectra were collected using a RQUINOX55 spectrometer. Sample powders were mixed with KBr by grinding, and then compressed into thin pellets for measurements. X-ray photoelectron spectroscopy (XPS) analysis was carried on a PHI-5000 VersaProbe X-ray photoelectron spectrometer. The dry sample powders were used for measurements. Raman spectra were collected using a J-YT640000, John Yvon Raman laser spectrometer using 514.5 nm laser excitation. The samples were placed on a clean glass slide for measurements. The crystalline phase and structure of powder samples were characterized by X-ray diffraction (XRD) using a D8-Advance, Bruker AXS diffractometer (Cu-Kα radiation, $\lambda = 1.5418$ Å, 40 kV, 100 mA, from $2\theta = 5$–80°, scan-speed 0.8 s/step, and increment of 0.02 deg/s). The morphology and microstructure were characterized by optical microscopy, field emission scanning electron microscopy (FESEM, HITACHI S−4800), transmission electron microscopy (TEM, JEOL JEM−2100), and atomic force microscopy (AFM**,** Bruker, Autoprobe CP-Reaserch). Sample powders were dispersed on conductive tapes placed on alumium sample holders for SEM measurements. Specimens for TEM measurements were prepared by droping aqueous suspensions (~0.02 mg/mL) of sample powders onto carbon-coated copper grids and dried in air. Specimens for AFM measurements were prepared by dropping aqueous suspensions (~0.02 mg/mL) of sample on freshly cleaned Si wafers and dried under vacuum at 70°C. Thermogravimetric analyses (TGA) were performed on a NETZSCH STA 449C thermogravimetric analyzer. The samples (~12 mg) were heated in N_2 atmosphere from room temperature to 900°C at 10°C/min.

Results and Discussion

Time-dependent UV-Vis absorption spectra were used to investigate the reduction process of GO suspensions for the five reductants (L-AA, D-fructose, glucose, sucrose, and Na_2SO_3). Pure GO has a maximum absorption peak at 228 nm, attributed to the π-π^* transition of the C═C bond, and a small absorption peak at 300 nm.[34] Pure graphene exhibits only one maximum absorption peak at 264 nm. During the reduction process of GO, a red-shift of the maximum absorption peak is observed due to restoration of the perfect sp^2 conjugated lattice system.[27,34] Thus, the red-shift of maximum absorption peak in the time-dependent UV-Vis absorption spectra can be used to determine the reduction rate by different reductants. In a typical chemical reduction process using L-AA as the reductant, the reaction solution was stirred at 95°C and from which a small amount of sample was withdrawn intermittently after 0, 5, 10, 30, 60, 120, and 240 min for UV-Vis absorption analysis. Figure 1A shows the time-dependent UV-Vis absorption spectra of the samples. At 0 min, the UV-Vis absorption spectrum shows a main peak at 228 nm and a very small peak at 300 nm originating from

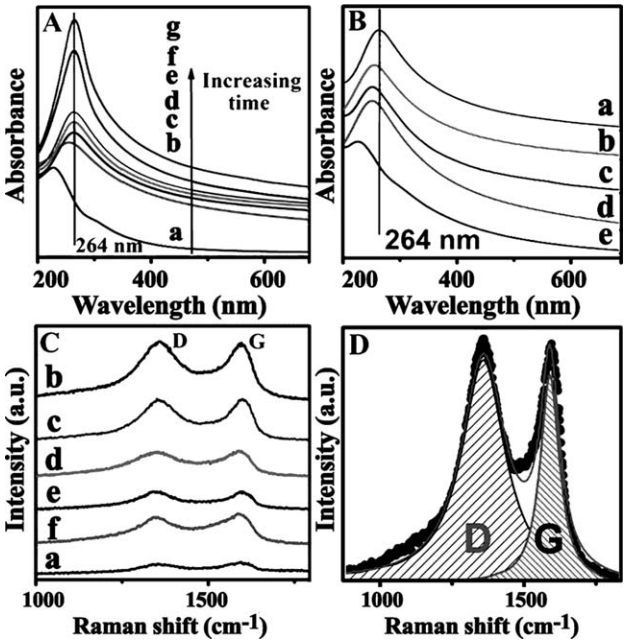

Figure 1. (A) UV-Vis absorption spectra of GO suspensions as a function of reduction time varying from (a) 0 to (b) 5, (c) 10, (d) 30, (e) 60, (f)120, and (g) 240 min in the presence of L-AA; (B) UV-vis absorption spectra of GO suspension reduced for 10 min by (a) L-AA, (b) D-fructose, (c) sucrose, (d) glucose, and (e) Na_2SO_3; (C) Raman spectra of (a) GO and those reduced by (b) L-AA for 10 min, (c) Na_2SO_3 for 4 h, (d) glucose for 1 h, (e) sucrose for 1 h, and (f) D-fructose for 30 min; (D) representative fitting curve of Raman spectrum of graphene completely reduced by L-AA for 10 min shown in Figure 1C-b.

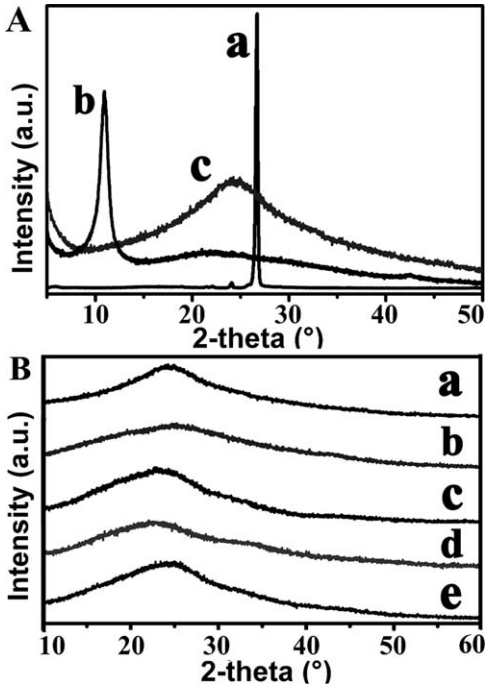

Figure 2. (A) XRD patterns of (a) graphite, (b) GO, and (c) reduced GO; (B) XRD patterns of reduced GO by (a) D-fructose, (b) sucrose, (c) glucose, (d) Na_2SO_3, and (e) L-AA.

pure GO. After 10 min of reduction, the main absorption peak red-shifts from 228 to 264 nm, indicative of transformation to mostly graphene. Beyond 10 min, no further shift of the absorption peak is observed, but the peak intensity increases with increasing reaction time, suggesting increasing density of graphitic domains in the suspension. The time-dependent reduction by the other four reductants (D-fructose, glucose, sucrose, and Na_2SO_3) was also investigated using the same method. As seen in Supporting Information Figure S1, the GO can be reduced within 0.5, 1, 1, and 4 h by D-fructose, glucose, sucrose, and Na_2SO_3, respectively. The major difference among the reductants is observed during the first 10 min of reaction. The main absorption peak shifts to 264 nm for L-AA, 256 nm for D-fructose, 252 nm for glucose, 254 nm for sucrose, and 228 nm for Na_2SO_3, as indicated by Figure 1B. Thus, the efficiency of reduction for the five reductants decreases in the order: L-AA > D-fructose > sucrose > glucose > Na_2SO_3.

Raman spectroscopy is a powerful tool to characterize the structure and electron conjugation state of carbon materials.[35,36] Two characteristic bands, G band at approximately 1575 cm^{-1} and D band at approximately 1355 cm^{-1}, are usually observed in graphitic carbon materials.[35] The G band is a doubly degenerate phonon mode (E_{2g} symmetry) at the Brillouin zone center that is Raman active for sp^2 carbon networks. Only a single G band is observed for highly crystalline graphite.[37] In contrast, the D band is the breathing mode of six-atom rings and requires defect for its activation. This defect-induced Raman feature is observed in defective and nanocrystalline samples.[38] A higher Raman D/G peak area ratio I_D/I_G is always observed for chemically reduced exfoliated GO and is generally attributed to a decrease of the average size of the sp^2 domain.[24,32,35] This I_D/I_G ratio has been used to compare the sp^2 graphite domain size for the different reductants as a measure of their effectiveness.[32,36] Figure 1C shows the Raman spectra of GO and reduced GO after reduction by L-AA (10 min), D-fructose (30 min), glucose (1 h), sucrose (1 h), and Na_2SO_3 (4 h). As compared to the spectrum of pristine graphite,[35,36] each sample exhibits a broader G band and an additional D band, the intensity of which depend on the degree of reduction of the sample. For a more quantitative comparison, I_D/I_G was calculated after curve fitting of the spectra (Figure 1D and Supporting Information Figure S2). The calculated I_D/I_G values are 1.21 for GO, 1.83 for D-fructose, 2.25 for sucrose, 2.46 for glucose, 2.51 for Na_2SO3, and 2.82 for L-AA. Assuming that an increase in the I_D/I_G ratio implies a decrease in the average size of in-plane sp^2 graphite domains, the average graphitic domain size in these samples follows the order: L-AA < Na_2SO_3 < glucose < sucrose < D-fructose. As L-AA is the most effective reductant, these results suggest that L-AA produces the most abundant and smallest graphitic domains amongst all five reduced GO samples.[32,36]

The crystal structure and phase purity of the reduced GO samples were characterized by XRD. As shown in Figure 2A-a, the XRD pattern of the pristine graphite shows an intense diffraction peak at $2\theta = 26.70°$, corresponding to an interlayer space of about 3.36 Å. For the GO (Figure 2A-b), only a peak at $2\theta = 10.92°$ is observed which corresponds to much larger interlayer spacing of 7.96 Å. This is caused by

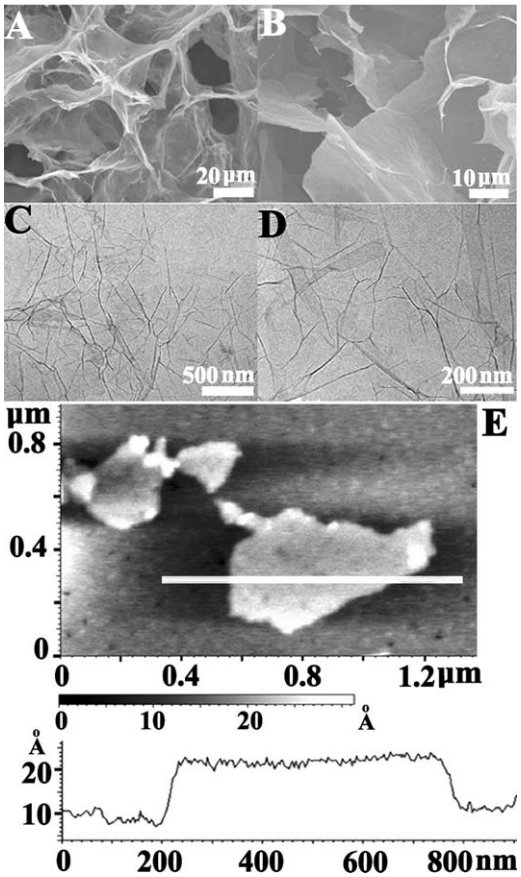

Figure 3. (A, B) SEM and (C, D) TEM images of L-AA reduced GO, (E) AFM image and corresponding height profile of an individual L-AA reduced GO sheet.

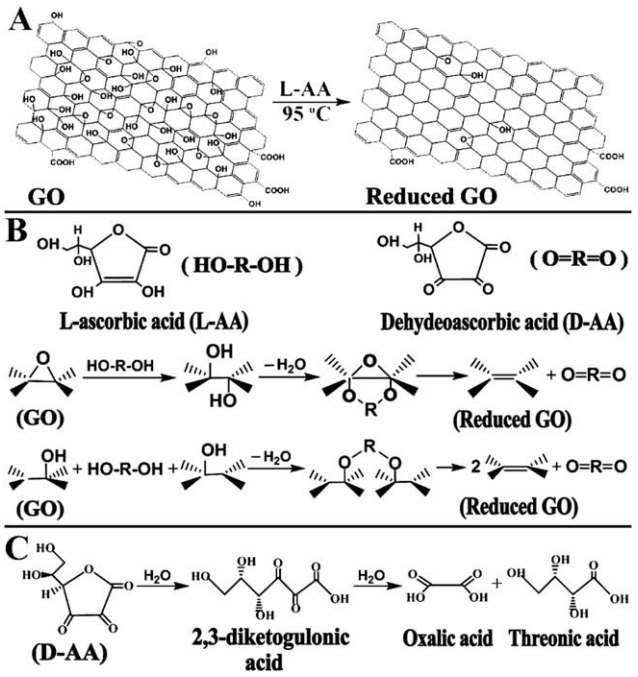

Figure 4. Schematic illustration of (A) redox reaction of GO, (B) proposed reaction pathway for the reduction reaction of GO in the presence of L-AA, and (C) proposed decomposition reaction pathway of dehydroascorbic acid.

the expansion of the interplanar spacing during the oxidation of graphite.[39] Also, the peak is broader than the graphite peak because of a distribution of interlayer spacings. The reduced GO (Figure 2A-c) shows a new broad diffraction peak at 24.94° (2θ) corresponding to the large d-spacing of 3.87 Å, while the characteristic peak of GO completely disappears. This implies substantial contraction of the interlayer spacing, presumably due to removal of the oxygen-containing functional groups on GO and recovery of graphitic domains and partial restoration of the graphitic structure. The d-spacing (3.87 Å) for the reduced GO is larger than that for graphite (3.36 Å) because of the presence of physical and/or chemical defects that prevent perfect π-π stacking of graphene sheets and incomplete removal of oxygen groups. Figure 2B shows the XRD patterns of reduced GO samples prepared using the five reductants. The positions of the diffraction peaks are 22.96° for glucose, 23.62° for Na_2SO_3, 24.26° for D-fructose, 24.94° for L-AA, and 25.28° for sucrose.

The morplology, size, and thickness of graphene sheets reduced by L-AA were examined by SEM, TEM, and AFM. Figures 3A, B are the SEM images of reduced GO sheets obtained from the suspension reduced by L-AA, showing lateral sizes around 100 to 200 μm. Figures 3C, D are the TEM images of the reduced GO sheets. Corrugations and scrollings are observed on the plane of reduced GO sheets. The high transparency of the sample suggests very thin layers. Figure 3E shows an AFM image and the height profile of one reduced GO sheet obtained by depositing an aqueous dispersion on a freshly cleaved mica surface through a drop-casting method. A very uniform contrast is observed throughout the entire sample. The thickness of this reduced GO sheet, measured from the height profile, is about 0.9 nm, indicating single layer graphene.[32]

The UV-Vis spectra (Figures 1A, B) indicate that L-AA could reduce GO significantly in a very short time of 10 min, much faster than the other four reductants. Moreover, significant differences in the reduction by L-AA with and without the addition of ammonia were observed. To further investigate the influence of ammonia on the reduction by L-AA, controlled experiments in the presence of either L-AA or ammonia were performed under the same reaction conditions. Using L-AA alone, the absorption peak shifted from 228 to 264 nm 1 h after initiating the reaction (Supporting Information Figure S3A). Using ammonia alone, only a very small red-shift was observed in the UV-Vis absorption spectra for the first 4 h (Supporting Information Figure S3B). It has been reported that GO contains several function groups including epoxide, hydroxyl, carbonyl, and carboxyl groups (Figure 4A),[24] and ammonia is known to be able to remove the oxygen-containing functional groups during the GO reduction.[40] When ammonia was added together with L-AA, the reduction of GO was much faster, as confirmed by the UV-Vis spectra (Figure 1A). However, this enhancement was not found for the other four reductants. We speculate that the kinetics of GO reduction by L-AA is changed by the presence of ammonia. In the reduction of GO, L-AA is oxidized to dehydroascorbic acid (Figure 4B), which is readily converted to 2, 3-diketogulonic acid, an intermediate product that can immediately be oxidatively degraded to oxalic acid and threonic acid (Figure 4C). In the presence of basic ammonium hydroxide, these intermediate acids can be

Figure 5. Photographs of aqueous suspensions of reduced GO, from left to right, reduced by L-AA, D-fructose, sucrose, glucose, and Na_2SO_3 after storage for 1 month.

[Color figure can be viewed in the online issue, which is available at wileyonlinelibrary.com.]

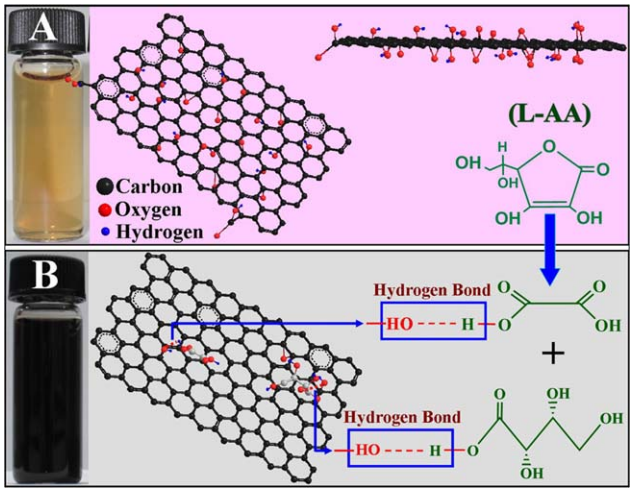

Figure 6. Schematic illustration of dispersion mechanism of well-dispersed L-AA reduced GO suspension: (A) the GO aqueous solution and (B) the uniform reduced GO aqueous suspension.

[Color figure can be viewed in the online issue, which is available at wileyonlinelibrary.com.]

neutralized rapidly, preventing buildup of the dehydroascorbic acid product and facilitating the reduction process. Supporting Information Figure S4 summarizes minimum times required for reduction of GO in the presence of different reductants.

The stability of the reduced GO suspension produced by the five reductants is indicated in Figure 5, taken after the samples were stored under laboratory ambient conditions for one month. Among the five samples, only the one reduced by L-AA remained in a stable suspension without any evidence of agglomeration. In fact, the sample was stable for months. Such ultrastability is beneficial for storage for later processing and modifications for applications. All the other four suspensions showed signs of agglomeration, and the sample reduced by Na_2SO_3 had settled completely to the bottom, most likely due to the salting effect.[27] In fact, precipitation was observed for the sample using Na_2SO_3 right after completion of the reduction process. For the samples reduced by the sugars, segregation was observed about 1 week later. Previous reports suggested that the surface of reduced GO is negatively charged due to the presence of residual carboxylic acid and the electrostatic charge repulsion between reduced GO sheets can stabilize the suspension.[27] The type and density of surface charge and the interface interaction can be controlled by tuning the zeta potential and pH value of the reduced GO suspension. It was found that the Zeta potential decreases from -30 to -43 mV with increasing pH value from 6.1 to 10. As the Zeta potential was adjusted to be more negative than -30 mV using ammonia, the reduced GO suspension maintained stability for over 2 days because of sufficient mutual repulsion. Thus, -30 mV is generally considered to be the critical value of the zeta potential that allows the reduced GO suspension to maintain stability.[27]

In our experiments, only the L-AA reduced GO exhibited ultrastability and the addition of ammonia had no detectable effect on the stability of the five suspensions. We assume that the L-AA molecules on addition intercalate into the GO sheets, form hydrogen bonds with surface hydroxyl and carboxyl groups on the GO, and reduce GO as well; during the reduction process, more acids derived from L-AA (Figure 4B, C), including excess L-AA, dehydroascorbic acid, 2,3-keketogulnol acid, oxalic acid, and threonic acid, provide a large number of hydroxyl groups and carboxyl groups that also may form hydrogen bonds with the residual oxygen functionalities, such as hydroxyl groups and periphery carboxylic groups, on the reduced GO (Figure 6). Such interactions bring charged groups and steric bulk to the surface of both the GO and the reduced GO, hindering π-π stacking between graphene sheets and preventing the formation of aggregates, and thus results in the ultrastability of reduced GO suspension.

We further investigated the oxygen functionalities on the reduced GO by FT-IR spectroscopy. Prior to reduction, GO contained large quantities of oxygen-containing functional groups. As shown in Figure 7A, peaks at $\sim$3426 and $\sim$1384 cm^{-1} are assigned to O—H stretching vibration and O—H deformation of hydroxyl group, respectively.[41,42] Peaks at $\sim$1758, $\sim$1195, and $\sim$1035 cm^{-1} are assigned to carboxyl (C=O stretching vibration), epoxy (epoxy C—O stretching vibration), and alkoxy functional groups (alkoxy C—O stretching vibration), respectively.[41,42] A C=C peak at 1677 cm^{-1} is due to the remaining carbon sp^2.[43] Figure 7B shows the FT-IR spectrum of as-reduced GO by L-AA. The reduced GO solution was centrifuged at 15,000 rpm and redispersed in water by rigorous shaking for two cycles to remove excess L-AA and its oxidation products before the FT-IR measurement. Significant decrease in peak intensities is observed for the C=O stretch (1758 cm^{-1}), epoxy C—O stretch (1195 cm^{-1}), and alkoxy C—O stretch (1035 cm^{-1}), which indicates most of the oxygen-containing functional groups formed on the GO during the oxidation of graphite are removed during the reduction process of GO using L-AA as reductant. A very intense, broad peak in the 3000–3700 cm^{-1} region suggests the presence of hydrogen-bonded hydroxyl groups, possibly from a combination of residual hydroxyl on the reduced GO, residual water, and adsorbed oxidation products of L-AA. The latter is consistent with the presence of the C—H stretch vibration at around 2900 cm^{-1}. Figure 7C shows the FT-IR spectrum of the L-AA reduced GO that was further cleaned by ultrasonic treatment

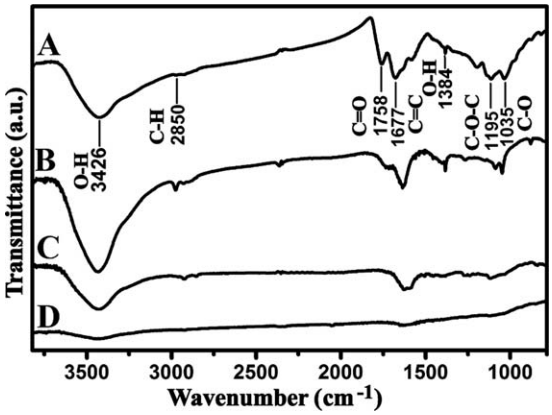

Figure 7. FT-IR spectra of (A) GO, (B) L-AA reduced GO after centrifugation two times without any ultrasonic treatment. (C) L-AA reduced GO after centrifugation five times with ultrasonic treatment, and (D) pristine graphite.

(operation power: 2000 W, operation frequency: 40 kHz) in water for 1 h and then centrifugation at 15,000 rpm for five cycles.[20] The FT-IR peaks corresponding to O—H deformation, C=O stretching vibration, epoxy C—O stretching vibration, and alkoxy C—O stretching vibration are much weaker. Meanwhile, the peak intensity for the O—H stretching vibration is dramatically decreased, although the C—H stretch is still readily observable. These observations confirm that the excess L-AA and the oxidation products of L-AA absorbed on the surface of the reduced GO can be detached from the reduced GO by the additional ultrasonic treatment and eventually removed by high-speed centrifugation. The above results indicate the presence of residual oxygen functionalities, adsorbed oxidation products of L-AA, and excess L-AA molecules on the surface of reduced GO that is rather stable.

For comparison, the FT-IR spectrum of pristine graphite was also investigated. As shown in Figure 7D, no obvious characteristic peaks are observed, which further indicates the presence of oxygen functionalities on the L-AA reduced GO sheets. The FT-IR spectra of the other four reduced GO samples are shown in Supporting Information Figure S5. For all the reduced GO samples, the intensities of the bands associated with oxygen functional groups and hydroxyl groups are decreased as compared to GO (Figure 7A). The L-AA reduced sample exhibits the most significant decrease in peak intensity, confirming its highest reducing ability among

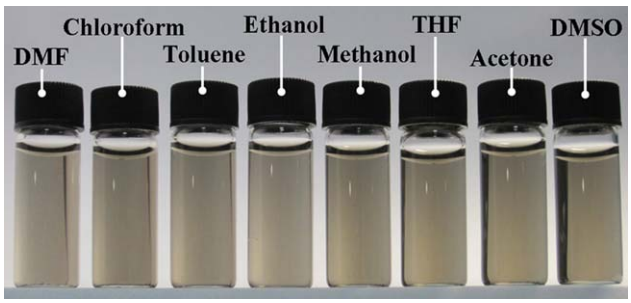

Figure 8. Digital image of as-prepared reduced GO dispersed in eight types of polar and nonpolar organic solvents.

[Color figure can be viewed in the online issue, which is available at wileyonlinelibrary.com.]

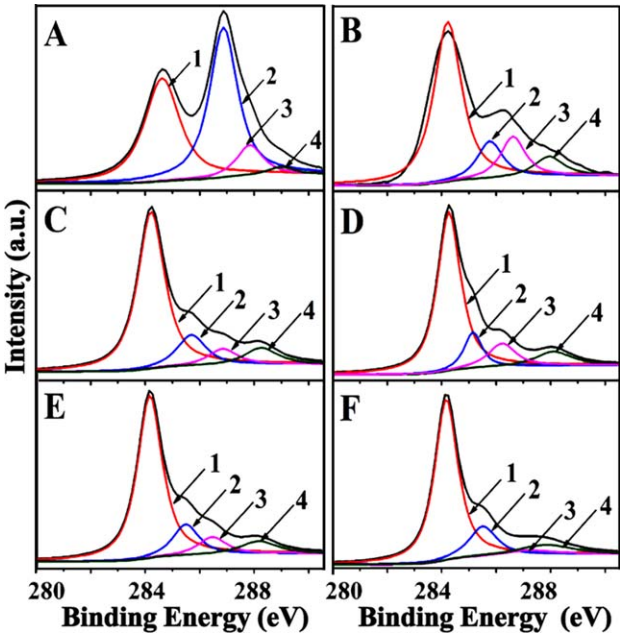

Figure 9. XPS spectra of C1s of (A) GO, reduced GO by (B) sucrose, (C) Na_2SO_3, (D) D-fructose, (E) glucose, and (F) L-AA. The peaks 1, 2, 3, and 4 correspond to C=C/C—C in aromatic rings, C—O (epoxy and alkoxy), C=O, and COOH groups, respectively.

[Color figure can be viewed in the online issue, which is available at wileyonlinelibrary.com.]

all the investigated reductants. The L-AA reduced GO can be dispersed not only in water but also in other polar or nonpolar organic solvents such as toluene, chloroform, tetrahydrofuran, acetone, dimethyl formamide (DMF), ethanol, methanol, and dimethylsulfoxide to form a stable suspension for months (Figure 8).

We postulate that such unusual amphiphilic property of L-AA reduced GO is determined by the balance between hydrophobicity arising from the reduced sp^2 graphite domains and hydrophilicity resulting from residual oxygen functionalities, the adsorbed excess L-AA and oxidization products of L-AA. The current method using L-AA as reductant produces the reduced GO that possesses the highest level of intrinsic properties of graphene. Most of oxygen-containing functional groups on the original GO can be removed during the reduction process. Therefore, the reduced GO has strong hydrophobicity that enables them to be easily dispersed in nonpolar solvents, such as toluene and chloroform. Conversely, the excess L-AA and oxidation products of L-AA contain abundant chemical functionalities that can form hydrogen bonds with the residual carboxyl and hydroxyl groups on the reduced GO and, thus, largely enhance the hydrophilic characteristic of the reduced GO. As a result, the L-AA reduced GO can also readily form stable dispersions in water and many polar solvents including tetrahydrofuran, acetone, DMF, ethanol, methanol, and dimethylsulfoxide. The unusual amphiphilic property of the L-AA reduced GO allows to prepare well-dispersed suspensions of the reduced GO in polar or nonpolar solvents, which provides versatile platforms for making transparent conductive thin films, functional nanocomposites, specialty coatings, carriers in biomedicine, conductor or catalyst supports for energy conversion and storage and so forth. This is very

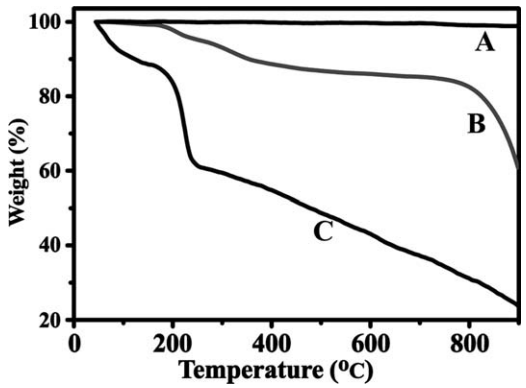

Figure 10. TGA curves in N_2 of: (A) pristine graphite, (B) L-AA reduced GO, and (C) GO.

important for future manipulation and processing of this unique material for many practical applications.

The degree of reduction of the reduced GO by the five different reductants was further characterized by XPS. As shown in Figure 9A, the C1s XPS spectrum of GO clearly indicates a considerable degree of oxidation with four different peaks at 284.5, 286.6, 287.8, and 289.0 eV, corresponding to C═C/C—C in aromatic rings, C—O (epoxy and alkoxy), C—O, and COOH groups, respectively.[24] After the reduction, the intensities of XPS peaks of the carbon atoms bonded to oxygen in all five reduced GO are significantly decreased, indicating that most of the oxygen-containing functional groups were removed after the reduction (Figures 9B–F). The oxygen to carbon (O:C) ratios deduced from corresponding XPS data are ~0.5 for GO, ~0.06 for L-AA reduced GO, ~0.09 for glucose reduced GO, ~0.11 for D-fructose reduced GO, ~0.18 for Na_2SO_3 reduced GO, and ~0.23 for sucrose reduced GO. The derived O:C atomic ratio indicates the presence of residual oxygen even on the reduced GO significantly reduced by L-AA. These results are in agreement with the previous UV-Vis, Raman, and FT-IR spectra results. Based on the O:C ratios, the degree of reduction of the reduced GO by five different reductants decreases in the order: L-AA > glucose > D-fructose > Na_2SO_3 > sucrose. The O:C ratio of the L-AA reduced GO rapidly decreases to 0.06 within only 10 min, much smaller than those of the other four samples, unambiguously confirms that L-AA is a highly efficient reductant for GO.

Another remarkable property of the L-AA reduced GO is its high-thermal stability. Figure 10 shows the TGA curves of pristine graphite, GO, and L-AA reduced GO. Pristine graphite (curve A) does not show any mass loss during the whole heating process. GO (curve C) exhibites the largest mass loss attributed to both evaporation of absorbed water and the removal of thermally labile oxygen functional groups.[24,44] In contrast, the L-AA reduced GO (curve B) does not show significant mass loss below 200°C, indicating that the sample does not contain a significant amount of adsorbed water. There is a 10% weight loss between ~200 and ~600°C, most likely due to loss of oxygen-containing functional groups of GO. Comparing to a loss of 30–40% for GO, a substantial portion of oxygen-containing functional groups must have been removed during the chemical reduction process and subsequent ultrasonic treatment. As described previously, the oxygen-containing functional groups include both those formed on the GO during the oxidation of graphite, the excess L-AA and oxidation products of L-AA absorbed on the surface of the reduced GO during the reduction process of GO. The former oxygen-containing functional groups on the original GO can be removed by chemical reduction. The latter excess L-AA and oxidation products of L-AA absorbed on the surface of the reduced GO can be detached from the reduced GO by a subsequent ultrasonic treatment and finally removed by high-speed centrifugation. Therefore, not only the reduction process but also the ultrasonic treatment can work for removing oxygen-containing functional groups. The origin of the significant weight loss above 800°C is not known. It could be due to pyrolysis of the carbon skeleton or loss of decomposed adsorbed excess L-AA and its oxidation products. A comparison of TGA curves of GO reduced by L-AA with those by the other four reductants (Supporting Information Figure S6) suggests that L-AA is indeed the most effective reductant, consistent with the previous UV-Vis, Raman, FT-IR, and XPS analysis.

Conclusions

In summary, we have described a green and efficient solution-phase chemical reduction method to prepare high-quality-reduced GO using L-AA as reductant. The reduction was rapid and essentially complete within 10 min. L-AA was more effective than D-fructose, glucose, sucrose, or Na_2SO_3. Very interestingly, the resulting reduced GO formed very stable suspensions in a variety of nonpolar and polar solvents. This enables the material to be easily modified for a broad of potential applications, such as composites, biomedicine, conductive inks, and energy storage and conversion. This eco-friendly process may provide a distinct advantage for large-volume production of graphene, and may enable important commercial development of the material.

Acknowledgments

This research was supported by the Natural Science Foundation of China (No. 21006044, No. 51202110), the Natural Science Foundation of Jiangsu Province (No. BK2012426, No. BK2012041), and the Project Funded by the Priority Academic Program Development of Jiangsu Higher Education Institutions (PAPD). H.H.K. is supported by the US DOE through the Center for Electrical Energy Storage (DE-AC-02-06CH11357). The authors thank the editor and referees for their critical comments and suggestions and Prof. Dr. Arunava Gupta of the MINT Center, The University of Alabama, for improving the English usage of the manuscript.

Literature Cited

1. Novoselov KS, Geim AK, Morozov SV, Jiang D, Zhang Y, Dubonos SV, Crigorieva IV, Firsov AA. Electric field effect in atomically thin carbon films. *Science*. 2004;306:666–669.
2. Geim AK, Novoselov KS. The rise of graphene. *Nat Mater*. 2007;6:183–191.
3. Allen MJ, Tung VC, Kaner RB. Honeycomb carbon: a review of graphene. *Chem Rev*. 2010;110:132–145.
4. Sui Y, Appenzeller J. Screening and interlayer coupling in multilayer graphene field-effect transistors. *Nano Lett*. 2009;9:2973–2977.
5. Cao A, Liu Z, Chu SS, Wu MH, Ye ZM, Cai ZW, Chang YL, Wang SF, Gong QH, Liu YF. A facile one-step method to produce graphene–CdS quantum dot nanocomposites as promising optoelectronic materials. *Adv Mater*. 2010;22:103–106.
6. Guo SJ, Wen D, Zhai YM, Dong SJ, Wang EK. Platinum nanoparticle ensemble-on-graphene hybrid nanosheet: one-pot, rapid synthesis, and used as new electrode material for electrochemical sensing. *ACS Nano*. 2010;4:3959–3968.

7. Schedin F, Geim AK, Morozov SV, Hill EW, Blake P, Katsnelson MI, Novoselov KS. Detection of individual gas molecules adsorbed on graphene. *Nat Mater*. 2007;6:652–655.
8. Robinson JT, Perkins FK, Snow ES, Wei ZQ, Sheehan PE. Reduced graphene oxide molecular sensors. *Nano Lett*. 2008;8:3137–3140.
9. Wang Y, Shi ZQ, Huang Y, Ma YF, Wang CY, Chen MM, Chen YS. Supercapacitor devices based on graphene materials. *J Phys Chem C*. 2009;113:13103–13107.
10. Wang X, Zhi LJ, Müllen K. Transparent, conductive graphene electrodes for dye-sensitized solar cells. *Nano Lett*. 2008;8:323–327.
11. Stoller MD, Park SJ, Zhu YW, An JH, Ruoff RS. Graphene-based ultracapacitors. *Nano Lett*. 2008;8:3498–3502.
12. Wu JB, Becerril HA, Bao ZN, Liu ZF, Chen YS, Peumans P. Organic solar cells with solution-processed graphene transparent electrodes. *Appl Phys Lett*. 2008;92:263–302.
13. Zhang YP, Li HB, Pan LK, Lu T, Sun Z. Capacitive behavior of graphene–ZnO composite film for supercapacitors. *J Electroanal Chem*. 2009;634:68–71.
14. Lu XK, Yu MF, Huang H, Ruoff RS. Tailoring graphite with the goal of achieving single sheets. *Nanotechnology*. 1999;10:269–272.
15. Kim KS, Zhao Y, Jang H, Lee SY, Kim JM, Kim KS, Ahn J-H, Kim P, Choi J-Y, Hong BH. Large-scale pattern growth of graphene films for stretchable transparent electrodes. *Nature*. 2009;457:706–710.
16. Pan Y, Zhang HG, Shi DX, Sun JT, Du SX, Liu F, Gao H-J. Highly ordered, millimeter-scale, continuous, single-crystalline graphene monolayer formed on Ru (0001). *Adv Mater*. 2009;21:2777–2780.
17. Sutter PW, Flege JI, Sutter EA. Epitaxial graphene on Ruthenium. *Nat Mater*. 2008;7:406–411.
18. Kosynkin DV, Higginbotham AL, Sinitskii A, Lomeda JR, Dimiev A, Price BK, Tour JM. Longitudinal unzipping of carbon nanotubes to form graphene nanoribbons. *Nature*. 2009;458:872–876.
19. Jiao LY, Zhang L, Wang XR, Diankov G, Dai H. Narrow graphene nanoribbons from carbon nanotubes. *Nature*. 2009;458:877–880.
20. Zhang WN, He W, Jing XL. Preparation of a stable graphene dispersion with high concentration by ultrasound. *J Phys Chem B*. 2010; 114:10368–10373.
21. Su Q, Pang SP, Alijani V, Li C, Feng XL, Müllen K. Composites of graphene with large aromatic molecules. *Adv Mater*. 2009;21:3191–3195.
22. Wang HL, Robinson JT, Li XL, Dai HJ. Solvothermal reduction of chemically exfoliated graphene sheets. *J Am Chem Soc*. 2009;131: 9910–9911.
23. Park SJ, Ruoff RS. Chemical methods for the production of graphenes. *Nat Nanotechnol*. 2009;4:217–224.
24. Stankovich S, Dikin DA, Piner RD, Kohlhaas KA, Kleinhammes A, Jia YY, Wu Y, Nguyen ST, Ruoff RS. Synthesis of graphene-based nanosheets via chemical reduction of exfoliated graphite oxide. *Carbon*. 2007;45:1558–1565.
25. Schmidt EW. Hydrazine and Its Derivatives: Preparation, Properties, Applications. New York: Wiley-Interscience, 1984.
26. Si YC, Samulski ET. Synthesis of water soluble graphene. *Nano Lett*. 2008;8:1679–1682.
27. Li D, Muller MB, Gilje S, Kaner RB, Wallace GG. Processable aqueous dispersions of graphene nanosheets. *Nat Nanotechnol*. 2008; 3:101–105.
28. Tao DM. The production status of sodium sulfite in The United States. *Inorg Chem Ind*. 2005;267:23–23.
29. Harbertson JF, Yuan C, Mireles MS, Hanlin RL, Downey MO. Glucose, fructose and sucrose increase the solubility of protein–tannin complexes and at high concentration, glucose and sucrose interfere with bisulphite bleaching of wine pigments. *Food Chem*. 2013;138: 556–563.
30. Gao QJ. Application of vitamins for food processing. *Ingredients*. 2000;7:20–20.
31. Chen WF, Yan LF, Bangal PR. Chemical reduction of graphene oxide to graphene by sulfur-containing compounds. *J Phys Chem C*. 2010;114:19885–19890.
32. Gao J, Liu F, Liu YL, Ma N, Wang ZQ, Zhang X. Environment-friendly method to produce graphene that employs vitamin C and amino acid. *Chem Mater*. 2010;22:2213–2218.
33. Hummers WS, Offeman RE. Preparation of graphitic oxide. *J Am Chem Soc*. 1958;80:1339.
34. Clark BJ, Frost T, Russell MA. UV Spectroscopy: Techniques, Instrumentation, Data Handling/UV Spectrometry Group. London: Chapman & Hall, 1997.
35. Tuinstra F, Koenig JL. Raman spectrum of graphite. *J Chem Phys*. 1970;53:1126–1130.
36. Krishnamoorthy K, Veerapandian M, Yun K, Kim SJ. The chemical and structural analysis of graphene oxide with different degrees of oxidation. *Carbon*. 2013;53:38–49.
37. Pimenta MA, Dresselhaus G, Dresselhaus MS, Cançado LG, Jorio A, Saito R. Studying disorder in graphite-based systems by Raman Spectroscopy. *Phys Chem Chem Phys*. 2007;9:1276–1290.
38. Cancado LG, Jorio A, Ferreira EHM, Stavale F, Achete CA, Capaz RB, Moutinho MVO, Lombardo A, Kulmala TS, Ferrari AC. Quantifying defects in graphene via Raman Spectroscopy at different excitation energies. *Nano Lett*. 2011;11:3190–3196.
39. Song SH, Ko CH, Ahn W, Kim BJ, Croiset E, Chen Z, Nam SC. Selective dibenzothiophene adsorption on graphene prepared using different methods. *Ind Eng Chem Res*. 2012;50:7772–7783.
40. Fan XB, Peng WC, Li Y, Li XY, Wang SL, Zhang GL, Zhang FB. Deoxygenation of exfoliated graphite oxide under alkaline conditions: a green route to graphene preparation. *Adv Mater*. 2008;20: 4490–4493.
41. Chen D, Feng HB, Li JH. Graphene oxide: preparation, functionalization, and electrochemical applications. *Chem Rev*. 2012;112:6027–6053.
42. Fu YS, Chen HQ, Sun XQ, Wang X. Graphene-supported nickel ferrite: a magnetically separable photocatalyst with high activity under visible light. *AIChE J*. 2012;52(11):3298–3305.
43. Su XQ, Wang G, Li WL, Bai JB, Wang H. A simple method for preparing graphene nano-sheets at low temperature. *Adv Powder Technol*. 2013;24:317–323.
44. Paredes JI, Villar-Rodil S, Martínez-Alonso A, Tascón JMD. Graphene oxide dispersions in organic solvents. *Langmuir*. 2008;24: 10560–10564.

Manuscript received Dec. 18, 2013, and revision received May 11, 2014.